Bioorganic & Medicinal Chemistry Letters 21 (2011) 7416–7420

Contents lists available at SciVerse ScienceDirect

Bioorganic & Medicinal Chemistry Letters

journal homepage: www.elsevier.com/locate/bmcl

Pyrrolamide DNA gyrase inhibitors: Optimization of antibacterial activity and efficacy

Brian A. Sherer *, Kenneth Hull, Oluyinka Green, Gregory Basarab, Sheila Hauck, Pamela Hill, James T. Loch III, George Mullen, Shanta Bist, Joanna Bryant, Ann Boriack-Sjodin, Jon Read, Nancy DeGrace, Maria Uria-Nickelsen, Ruth N. Illingworth, Ann E. Eakin

Infection Innovative Medicines Unit, AstraZeneca R&D Boston, 35 Gatehouse Drive, Waltham, MA 02451, USA

ARTICLE INFO

Article history:
Received 8 August 2011
Revised 3 October 2011
Accepted 4 October 2011
Available online 12 October 2011

Keywords:
Antibacterial
Gyrase
Pyrrolamide

ABSTRACT

The pyrrolamides are a new class of antibacterial agents targeting DNA gyrase, an essential enzyme across bacterial species and inhibition results in the disruption of DNA synthesis and subsequently, cell death. The optimization of biochemical activity and other drug-like properties through substitutions to the pyrrole, piperidine, and heterocycle portions of the molecule resulted in pyrrolamides with improved cellular activity and in vivo efficacy.

The emergence of drug resistance in both community- and hospital-acquired infections has outpaced development and delivery of new antibacterial drugs to the clinic. As a result, there is a serious global health threat that currently available therapies will no longer be effective in treating bacterial infections.[1] One approach to combating the emergence of resistance to current antibacterial drugs is to discover novel agents that inhibit known drug targets through a unique binding site, chemistry or mechanism of inhibition; thereby evading existing resistance mechanisms developed by bacteria.

DNA gyrase has long been known as an attractive target for antibacterial drugs.[2] DNA gyrase is a member of the type II family of topoisomerases that control the topological state of DNA in cells.[3] It is a tetrameric enzyme comprised of two subunits each of GyrA and GyrB. DNA gyrase couples ATP hydrolysis by the GyrB subunit to negative supercoiling of DNA, which is required for maintenance of DNA topology during the replication process. DNA gyrase is an essential enzyme across bacterial species and inhibition results in a disruption of DNA synthesis and ultimately, cell death. Two classes of antibiotics have clinically validated DNA gyrase as a viable target—the fluoroquinolones and aminocoumarins. However, increasing prevalence of resistant bacterial strains is eroding the utility of these quite successful fluoroquinolone drugs.[4] The coumarin class of antibiotics have failed to achieve widespread utility because of poor pharmacokinetics and issues of safety.[5]

Previous efforts at AstraZeneca identified a novel class of DNA gyrase inhibitors—the pyrrolamides—using a fragment-based NMR screening approach followed by a structure-guided lead identification strategy.[6] The pyrrolamide series inhibits the enzyme by binding to the ATP pocket of GyrB, as demonstrated by an initial lead compound **1** (Fig. 1) with submicromolar enzyme potency but weak antibacterial activity. Compound **2** (Fig. 1) is a subsequent compound in the pyrrolamide series that displayed promising antibacterial activity and demonstrated in vivo efficacy against *S. pneumoniae* in a mouse pneumonia model.[7] Described herein is the elaboration of SAR for the pyrrolamide series that led to **2** and further optimization of the antibacterial potency to provide **26**, which resulted in improved in vivo efficacy over that of **2**.[7]

The synthesis of substituted pyrrolamide analogs is illustrated in Scheme 1. The previously reported ethyl 2-methyl-5-carboxylate pyrrole[8] was treated with either *N*-bromo or *N*-chlorosuccinimide followed by ester hydrolysis to obtain the 3-halosubstituted pyrroles **3** and **4**. Ethyl 5-methyl-1*H*-pyrrole-2-carboxylate was also subjected to sulfuryl chloride and followed by ester hydrolysis to provide the 3,4-dichlorosubstituted pyrrole **5**. A three step procedure from ethyl 5-methyl-1*H*-pyrrole-2-carboxylate to provide the corresponding aldehyde followed by formation of the hydroxylimine and dehydration gave the 3-cyanopyrrole **6**. Pyrroles **3**, **4**, **5**, and **6** were subjected to an amide coupling with commercially available *N*-Boc-4-aminopiperidine. Finally, Boc-deprotection was followed by nucleophilic substitution with commercially available 2,6-dichloropyridine-4-carboxamide to yield compounds **1**, **7**–**10**.

The synthetic sequence used to prepare the pyrrolamides **2** and **12**–**16** is described in Scheme 2. Amide coupling of

* Corresponding author. Tel.: +781839 4143.
E-mail address: brian.sherer@astrazeneca.com (B.A. Sherer).

0960-894X/$ - see front matter © 2011 Elsevier Ltd. All rights reserved.
doi:10.1016/j.bmcl.2011.10.010

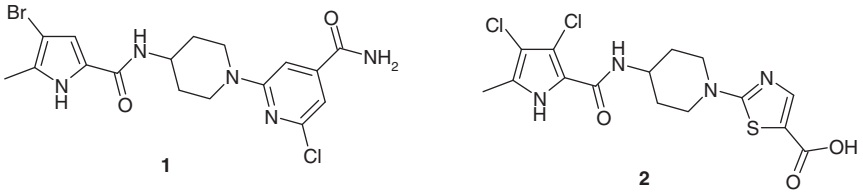

Figure 1. Structure of early lead compounds in the pyrrolamide series.

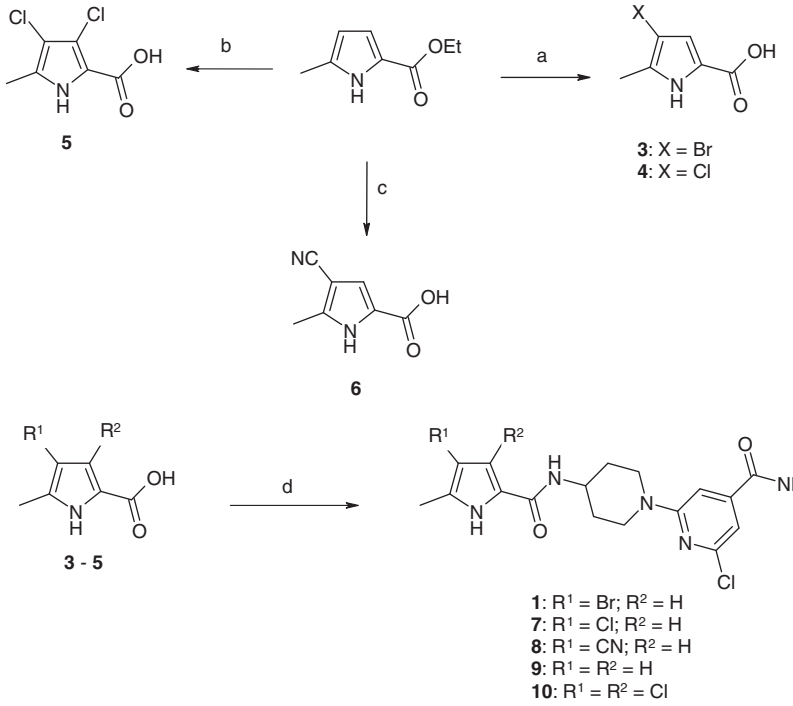

Scheme 1. Synthesis of substituted pyrrole compounds **1**, **7**–**10**. Reagents and conditions: (a) (1) *N*-bromosuccinimide or *N*-chlorosuccinimide 0 °C, 38–50%; (2) NaOH, MeOH, water, 70–92%; (b) (1) SO_2Cl_2, carbon tetrachloride, 77%; (2) NaOH, MeOH, water, 60–75%; (c) (1) trimethoxymethane, TFA, 45%; (2) hydroxylamine, ethanol then thionyl chloride, DMF, 0 °C 80%; (3) NaOH, MeOH, water, 70% (d) (1) HATU, DIPEA, DMF, *N*-Boc-4-aminopiperidine, 70–95%; (2) HCl, dioxane, 98%; (3) 2,6-dichloropyridine-4-carboxamide, 80 °C, 60–80%.

N-Boc-4-aminopiperidine and removal of the protecting group provided intermediate **11**. Nucleophilic substitution of the corresponding halo-heterocycle with piperidine **11** followed by hydrolysis of the ester yielded acids **2**, **12**–**13**. Compound **14** was analogously prepared by nucleophilic displacement of chloro-oxadiazole.[8b] A reductive amination of intermediate **11** and *trans*-hydroxyproline ester followed by basic hydrolysis provided pyrrolidine **15**. Formation of the amide from acid **2** under standard conditions yielded amide **16**.

The synthesis of 3-fluoropiperdine analogs is described in Scheme 3. Racemic *cis*- and *trans*-*N*-Boc-3-fluoro-4-benzylaminopiperidines (**18a**, **18b**) were prepared as described previously.[9] The benzyl protecting group was removed from **18a** and **18b** and the resulting amine was coupled to acid **5**. Deprotection of the piperidine, followed by nucleophilic substitution on methyl 2-bromothiazole-5-carboxylate, and ester hydrolysis led to racemic *cis*- and *trans*-acids **19** and **20**. Piperidine **18** was also subjected to chiral chromatography[10] to provide the pure *cis*-enantiomers **24** and **25**, which were then independently subjected to the reaction conditions described above to provide the enantiomerically pure analogs **26** and **27**. The absolute configuration of compound **26** was determined via small molecule X-ray crystallography to be (3*S*,4*R*).[11]

Shown in Table 1 are the results of efforts to improve both the enzyme and antibacterial activity[12] of lead compounds in the pyrrolamide series by changing the substituents on the pyrrole portion of the molecule.[13] The 3,4-dichloropyrrole **10** provided the best in vitro potency of 0.03 μM while the methyl pyrrolamide **9** had the weakest activity with an IC_{50} of 7 μM.[14] All of the 3-substituted pyrroles **1**, **7**–**9** had similar potencies of ~0.15 μM. The pyrrole group binds in the adenine binding pocket of GyrB forming hydrogen bond interactions with a conserved aspartic acid 82 residue and water molecule as shown in the X-ray co-crystal structure of **26** with the 24 kDa N-terminal ATP binding domain of GyrB that had previously been used for analyzing inhibitor complexes (Fig. 2).[15] The enhanced enzyme activity of compound **10** relative to **1**, **7**–**9** can be explained by the presence of two lipophilic electron withdrawing groups on the pyrrole, which increase hydrophobic interactions in the adenine pocket and decrease the pK_a of the pyrrole nitrogen resulting in a stronger hydrogen bond donation to the aspartate residue. The decreased activity of the pyrrole **9** confirms the hypothesis that an electron withdrawing group is preferred for increasing potency. The enzyme potency correlated well with the cellular activity as compound **10** displayed the best antibacterial activity particularly against Gram-positive bacteria. All the compounds

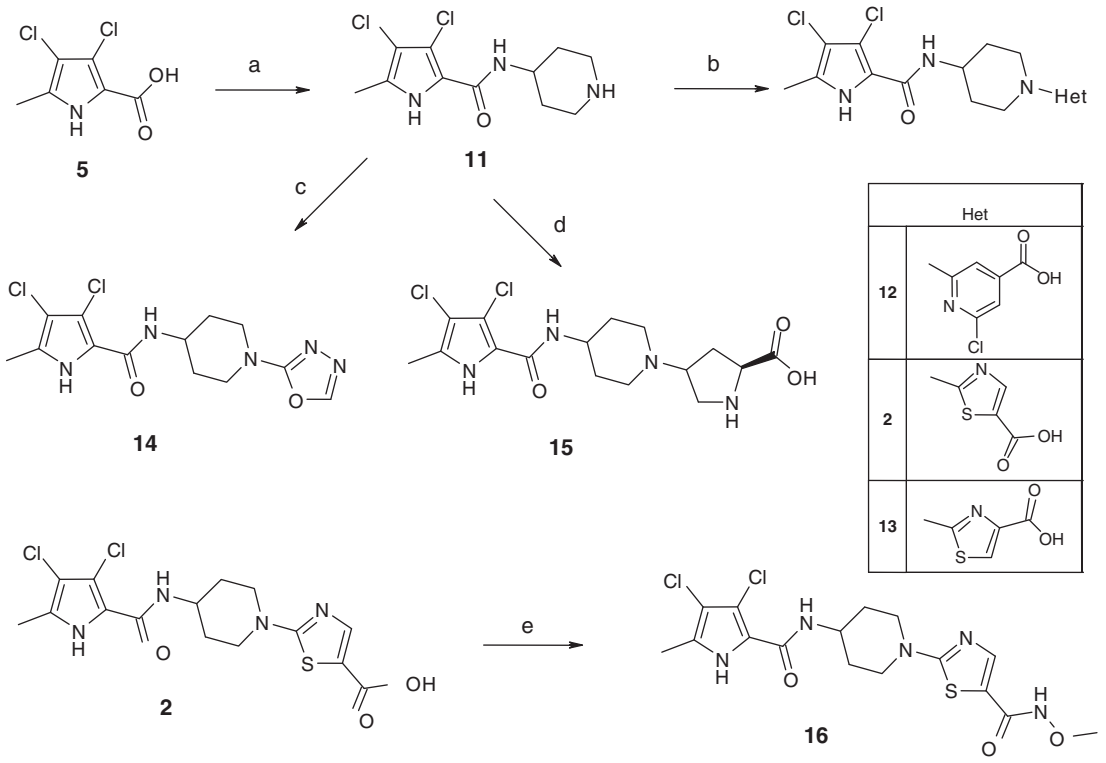

Scheme 2. Synthesis of heterocyclic compounds **2**, **12**–**16**. Reagents and conditions: (a) (1) HATU, DIPEA, *N*-Boc-4-aminopiperidine, DMF, 70–90%; (2) HCl, dioxane, 98%; (b) (1) DIPEA, DMF, methyl 2,6-dichloropyridine-4-carboxylate or methyl 2-bromothiazole-4-carboxylate or 2-bromothiazole-5-carboxylate, 80 °C, 63–79%; (2) NaOH, water, MeOH, 88%; (c) preparation according to ref 7a; (d) (1) *N*-Boc-*trans*-4-hydroxy-L-proline methyl ester, $NaCNBH_3$, 64% (2) HCl, dioxane, 95%; (3) NaOH, MeOH, water, 90%; (e) HATU, DIPEA, DMF, methoxylamine, 78%.

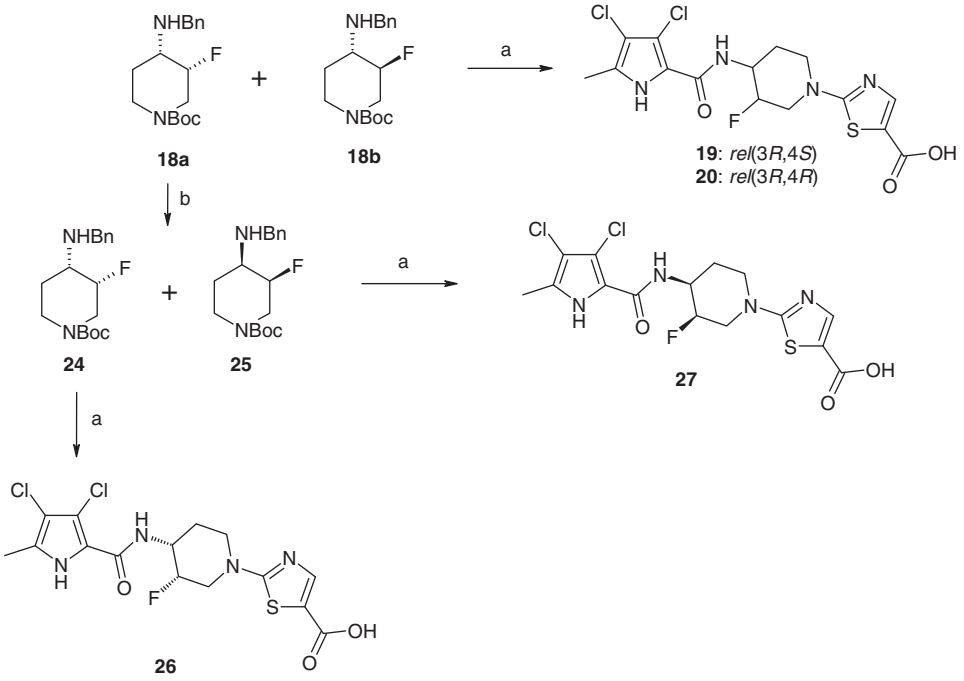

Scheme 3. Synthesis of 3-fluoropiperidines **19**, **20**, **26**, **27**. Reagents and conditions: (a) (1) **5**, H_2, Pd/C, MeOH, 82%; (2) HATU, DIPEA, DMF, 60%; (3) HCl, 1,4-dioxane, 95%; (4) methyl 2-bromothiazol-5-carboxylate, 65%; (5) NaOH, MeOH, water, 87%; (b) chiral chromatograp.

displayed significantly lower activity against the Gram-negative bacteria, *Haemophilus influenzae* and *Escherichia coli*. However, all of the 3-substituted pyrroles except **9** displayed activity against an efflux deficient strain of *E. coli* (*tolC*$^-$), suggesting that an efflux mechanism limits the Gram-negative potency of the more active DNA gyrase inhibiting compounds.

The structure activity relationships from efforts to further optimize enzyme and cellular potency by replacement of the

Table 1
Structure–activity relationship of pyrrole substitutions

Compd	*S. aureus* IC_{50} (μM)	Minimum Inhibitory Concentration (μg/mL)							
		S. pneumoniae	*S. aureus*	*S. aureus MRQR*[b]	*M. catarrhalis*	*E. faecium*	*H. influenzae*	*E. coli*	*E. coli tolC*⁻
1	0.10	4	32	32	8	>64	64	>64	4
7	0.11	4	>32	32	ND[a]	>32	>64	>64	8
8	0.15	4	ND	>64	ND	ND	>64	ND	ND
9	6.9	>64	>64	>64	>64	>64	>64	>64	>64
10	0.03	1	4	4	2	4	>64	>64	2

[a] ND = Not determined.
[b] MRQR = methicilin-resistant, quinolone resistant.

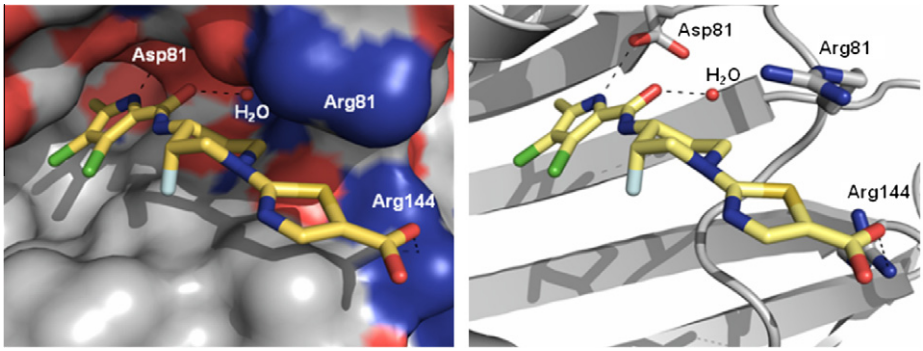

Figure 2. An X-ray structure of a 3-fluorosubstituted piperidine analog **26** with *S. aureus* GyrB displayed with surface (left) and stick (right) representations.

pyridine of **10** with other heterocycles are shown in Table 2. Five-membered ring heterocycles, such as thiazoles, displayed the best combination of physical properties and potency. Heterocycles **2**, **12**–**14**, and **16** all maintained enzyme potency in the low nanomolar range while compound **15** had weaker activity at the μM level. The heterocycles attached to the piperidine nitrogen extends outside of the ATP binding region, forming stacking and hydrogen bonding interactions with protein residues as shown in Figure 2. The aromatic nature of these heterocycles is key for optimizing pi-stacking with Arg84. The aromatic heterocycles of all the compounds except **15** are additionally substituted with carboxylate or carboxamide groups which form hydrogen bond interactions with Arg144 in the GyrB active site (Fig. 2). The lower enzyme potency for **15** is due in part from the lack of capability for the pi-stacking with Arg144 and in part from there being a poor alignment for the hydrogen bond between the carboxylate and Arg84. An enhancement in antibacterial spectrum of compounds **2** and **12**–**13** to include fastidious Gram-negative bacteria, such as *H. influenzae* and *Moraxella catarrhalis*, can potentially be attributed to an increase in cell permeability imparted by the presence of a carboxylate substituent on the heterocycle. Compounds such as **12** that maximize both stacking and hydrogen bond interactions outside of the ATP pocket and, additionally, that optimize the pyrrole hydrogen bond to Asp81 and that are hydrophobic in the ATP pocket generally show promising cellular activity against Gram-positive bacteria, including methicilin- and quinolone-resistant *S. aureus* and fastidious Gram-negative bacteria, such as *H. influenzae* and *M. catarrhalis*. Broader potency against enteric Gram-negative pathogens such as *E. coli* remains hampered by efflux, as demonstrated by improved potency against an efflux-deficient (*tolC*⁻) strain.

The piperidine moiety of the pyrrolamides was investigated to determine if any further improvements could be obtained in enzyme potency and antibacterial activity by incorporating a single fluorine substituent at the 3-position (Table 3).[16] The resultant stereochemical relationship between the 3-F and the 4-amide substituents on the piperidine proved to be crucial for improvement in potency with the racemic *cis*-piperidine **19** being 10–20 times more potent than the racemic *trans*-piperidine **20** in both enzyme and anti-bacterial activity. Furthermore, the enantiomerically pure (3*S*,4*R*) analog **26** displayed approximately eightfold greater potency over the (3*R*,4*S*) enantiomer **27** in both enzyme and cellular activities. Overall, the single fluorine atom incorporation in **26** improves activity 4–8 fold. The fluorine atom in **26** is directed towards a hydrophobic pocket in the GyrB active site (Fig. 2), which could account for the improvement in potency compared to unsubstituted analogs. Additionally, the fluorine atom could adjust the piperidine conformation to better align the pyrrole carboxamide

Table 2
Structure–activity relationship of heterocycle substitutions

Compd	*S. aureus* IC_{50} (μM)	Minimum Inhibitory Concentration (μg/mL)							
		S. pneumoniae	*S. aureus*	*S. aureus MRQR*	*M. catarrhalis*	*E. faecium*	*H. influenzae*	*E. coli*	*E. coli tolC*⁻
10	0.03	1	4	4	2	4	>64	>64	2
12	0.01	0.5	2	2	0.13	1	4	>64	0.25
2	0.0 2	0.5	8	8	0.5	2	2	>64	0.25
13	0.02	0.5	8	8	0.5	4	2	>64	0.25
16	0.05	1	8	8	1	8	16	>64	0.25
14	0.23	4	32	32	4	32	64	>64	4
15	129	>64	>64	>64	>64	>64	>64	>64	>64

Table 3
Structure–activity relationship of unsubstituted and 3-F substituted piperidines

Compd	*S. aureus* IC_{50} (μM)	Minimum Inhibitory Concentration (μg/mL)							
		S. pneumoniae	*S. aureus*	*S. aureus MRQR*	*M. catarrhalis*	*E. faecium*	*H. influenzae*	*E. coli*	*E. coli tolC*$^-$
2	0.02	0.5	8	8	0.25	2	2	>64	0.25
19	<0.01	0.13	2	4	<0.06	0.5	0.5	>64	0.13
20	0.11	8	>64	>64	16	32	64	>64	4
26	0.004	0.06	2	2	0.06	0.25	0.25	>64	0.06
27	0.035	2	16	32	1	4	4	>64	0.5

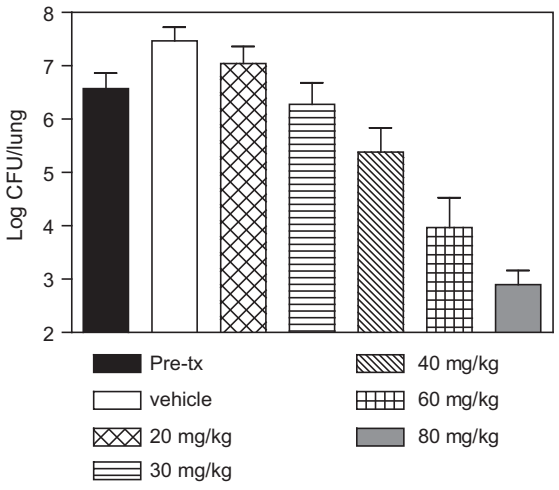

Figure 3. Dose–response effect on the treatment of mice with compound **26** in a *S. pneumoniae* lung infection model. Error bars represent standard error in the CFU measurements.

with Asp81 and the thiazole carboxylate with Arg84. The racemic *trans*-piperidine **20** showed weak activity relative to the unsubstituted analog **2** consistent with the *trans*-isomer changing the conformation of the piperidine ring and disrupting optimal stacking and hydrogen bonding interactions with the protein. The fluorine atom of the (3*R*, 4*S*) enantiomer **27** is orientated towards a less favorable interaction with the water molecule associated with Asp81 rather than towards the hydrophobic pocket as for the more active (3*S*, 4*R*) enantiomer.

Compound **26** was evaluated in vivo against *S. pneumoniae* in a mouse model of pneumonia (Fig. 3).[17] Compound **26** or vehicle was dosed orally starting 18 h post-infection and activity was quantified by viable counts on serial dilutions of lung homogenates 24 h after start of the treatment and presented in Figure 3 as mean log CFU/lung (+/- standard error) for each group of mice. Compound **26** was found to be efficacious against *S. pneumoniae* in this mouse model of pneumonia, causing a dose-dependent decrease in viable bacterial counts in the lung. A dose of 80 mg/kg resulted in the maximum response seen in this experiment and an ED_{50} was estimated to be 54 mg/kg. Overall, considerable improvement in efficacy was demonstrated with **26** relative to **2** (4× by dose for maximal effect), as reported previously,[7] in line with what would be anticipated with the greater antibacterial activity against the pathogen.

In conclusion, this Letter has presented the efforts at optimization of biochemical and cellular activity of a novel class of antibacterial agents, the pyrrolamides. Substitution on the piperidine moiety resulted in improvements in potency, which translated into in vivo activity in a lung model of infection. Further efforts to improve potency and decrease the dose required for efficacy are ongoing.

Acknowledgments

The authors thank the following individuals for valuable technical contributions to this project: Barbara Arsenault, John Breed, Amanda Doucette, Elise Gorseth, Grant Walkup, Bryan Prince, Linda Otterson, Lena Grosser, Susie Hopkins, Larry MacPherson, and Dedong Wu.

References and notes

1. (a) Boucher, H. W.; Talbot, G. H.; Bradley, J. S.; Edwards, J. E., Jr.; Gilbert, D.; Rice, B.; Scheld, M.; Spellberg, B.; Bartlett, J. *Clin. Infect. Dis.* **2009**, *48*, 1; (b) Talbot, G. H.; Bradley, J.; Edwards, J. E., Jr.; Gilbert, D.; Scheld, M.; Bartlett, J. *Clin. Infect. Dis.* **2006**, *42*, 657; (c) Alanis, A. J. *Arch. Med. Res* **2005**, *36*, 697.
2. Maxwell, A. *Trends Micro.* **1997**, *5*, 102.
3. Wang, J. C. *Untangling the double helix; DNA entanglement the action of the DNA topoisomerases*; Cold Spring Harbor Laboratory Press: Cold Spring Harbor, NY, 2009.
4. (a) Biedenbach, D. J.; Farrell, D. J.; Mendes, R. E.; Ross, J. E.; Jones, R. N. *Diagn. Microbiol. Infect. Dis.* **2010**, *68*, 459; (b) Rhomberg, P. R.; Jones, R. N. *Diagn. Microbiol. Infect. Dis.* **2009**, *65*, 414; (c) Boyd, L. B.; Atmar, R.; Randall, G.; Hanill, R.; Steffen, D.; Zechiedrich, L. B. M. C. *Infect. Dis.* **2008**, *8*, 4.
5. Maxwell, A. *Mol. Microbiol.* **1993**, *9*, 101.
6. Green, O.; Ni, H.; Singh, A.; Walkup, G.; Hales, N.; Breeze, A.; Eakin, A.E. 48th Annual Meeting of the Interscience Conference on Antimicrobial Agents and Chemotherapy, Washington, D.C. October 25–28, 2008, F1-2025.
7. Illingworth, R.N.; Uria-Nickelsen, M; Eakin, A.E. 48th Annual Meeting of the Interscience Conference on Antimicrobial Agents and Chemotherapy, Washington, D.C. October 25–28, 2008, F1-2028.
8. (a) Curran, T. P.; Keaney, M. T. *J. Org. Chem.* **1996**, *61*, 9068; (b) Breeze, A.L.; Green, O. M.; Hull, K. G.; Hauck, S. I.; Ni, H.; Mullen G. B.; Hales, N. J.; Timms, D. WO2005026149.
9. Van Niel, M. B.; Collins, I.; Beer, M. S.; Broughton, H. B.; Cheng, S. K. F.; Goodacre, S. C.; Heald, A.; Locker, K. L.; MacLeod, A. M.; Morrison, D.; Moyes, C. R.; O'Connor, D.; Pike, A.; Rowley, M.; Russell, M. G. N.; Sohal, B.; Stanton, J. A.; Thomas, S.; Verrier, H.; Watt, A. P.; Castro, J. L. *J. Med. Chem.* **1999**, *42*, 2087.
10. Chiral chromatography conditions: Chiralpak AD 500 × 50 mm, 20μ, 90% hexanes, 5% methanol, 5% ethanol, 0.1% diethylamine; flow rate: 118 ml/min.
11. X-ray coordinates deposited in Cambridge Crystallographic Data Centre #835685.
12. Minimum Inhibitory Concentration measurements performed according to Clinical and Laboratory Standards Institute, Wayne, PA on the following bacterial strains from the AstraZeneca collection: *Streptococcus pneumoniae* ARC548, *Staphylcoccus aureus* ARC516, *S. aureus* MRQR ARC517, *Moraxella catarrhalis* ARC445, *Enterococcus faecium* ARC073, *Haemophilus influenzae* ARC446, *Escherichia coli* ARC523, and *E. coli* tolC- ARC524.
13. Hull, K.; Green, O.; Singh, A.; Bist, S.; Demeritt, J.; Loch,J.; Mullen, G.; Hauck, S.; Sherer, B.; Ni, H.; Eakin, A. E., 48th Annual Meeting of the Interscience Conference on Antimicrobial Agents and Chemotherapy, October 24–28, 2008, F1-2027.
14. Inhibition of DNA gyrase by test compounds was measured using ammonium molybdate/malachite green-based phosphate detection assays performed in the presence of a range of concentrations of test compound. Assays of the *S. aureus* GyrB ATPase utilized a hybrid tetramer enzyme reconstituted *in vitro* from recombinant *S. aureus* GyrB and *E. coli* GyrA. The IC_{50} value is the concentration of compound required for 50% inhibition of the gyrase ATP-hydrolysis activity.
15. X-ray coordinates deposited in RSCB Protein Data Bank; PDB ID Code: 3TTZ.
16. Sherer, B.; Basarab, G.; Hull, K.; Hauck, S.; Bist, S.; Eakin, A. E. 49th Annual Meeting of the Interscience Conference on Antimicrobial Agents and Chemotherapy, San Francisco, CA, September 12–15, 2009, F1-1977.
17. The animals used for the mouse infection model were maintained in accordance with the criteria for the American Association for Accreditation of Laboratory Animal Care. The entire study was conducted using an IACUC-approved protocol in accordance with Title 9 of the Code of Federal Regulations. Groups of 10 CD1 mice (Charles River Laboratories, MA) were infected intratracheally with 10^5 CFU/lung of *S. pneumonia* ARC548, whilst under anesthesia with ketamine/xylazine.